Electroencephalography and clinical Neurophysiology, 1987, 66: 286–298
Elsevier Scientific Publishers Ireland, Ltd.

EEG 01797

Experimental Section

On the magnetic field distribution generated by a dipolar current source situated in a realistically shaped compartment model of the head

J.W.H. Meijs *, F.G.C. Bosch **, M.J. Peters ** and F.H. Lopes da Silva ***

* *Department of Electrical Engineering, and ** Department of Technical Physics, Twente University of Technology, 7500 AE Enschede (The Netherlands), and *** Biological Centre, University of Amsterdam, 1098 SM Amsterdam (The Netherlands)*

(Accepted for publication: 14 July, 1986)

Summary The magnetic field distribution around the head is simulated using a realistically shaped compartment model of the head. The model is based on magnetic resonance images. The 3 compartments describe the brain, the skull and the scalp. The source is represented by a current dipole situated in the visual cortex. The magnetic field distribution due to the source and that due to the volume currents are calculated separately. The simulations are carried out in order to ascertain which matrix of grid points is suitable as a measuring grid. The possibilities studied are grid points situated in a plane, in a surface which follows the contours of the head and in a sphere. This sphere is taken concentric to the sphere which is the best possible fit for the head. Taking into account the relative contribution of the volume currents and the possible accuracy in the positioning of the magnetic field detector, it can be concluded that the best choice is to measure the *normal* component of the magnetic field at points which are situated in the spherical surface. The results of this study also show that the magnetic field distribution based on a realistically shaped compartment model differs from that based on a compartment model consisting of concentric spheres. In the spherical model of the head no contribution of the volume currents to the component of the field normal to the sphere can be expected. The difference between the results obtained with these two volume conductor models increases with source depth.

Key words: magnetoencephalography; visual cortex; simulation; volume conductor shape; recording surfaces

The accuracy of source localization within the brain based on magnetoencephalographic (MEG) measurements around the head depends on the adequacy of the models used to represent both the source and the volume conductor (i.e., the head). The most commonly used model for a source is a single-current dipole or a current dipole layer. Up to now mathematical models of the head have been confined to spherical models (Cohen and Cuffin 1983), although the influence of the shape of an isolated human skull on the magnetic field was measured by Weinberg et al. (1984) and Barth et al. (1986).

In some cases the adequacy of a model used for the localization of a source may be confirmed, for instance, by X-ray tomographs in studies of focal epilepsy (Barth et al. 1984). However, in most other cases such a confirmation cannot be obtained. Although not conclusive, a model inspires confidence when source localization, using this model, leads to the same results when the localization is based on the measured EEG distribution as in the case where the localization is based on the measured MEG distribution.

For sources in the visual cortex the estimated source location based on the visual evoked potentials did not coincide with the location based on the visual evoked magnetic fields (Stok et al. 1984). The model used for the computations consisted of 4 concentric spheres, where the spheres were fitted in the section of the head near the visual cortex. Because the spherical model is not adequate to describe both EEG and MEG measurements simultaneously, better models have to be used of

Correspondence to: J.W.H. Meijs, Department of Electrical Engineering, Twente University of Technology, P.O. Box 217, 7500 AE Enschede, The Netherlands.

either the volume conductor or the source. Therefore a more realistically shaped model of the head was used in this study.

The magnetic field distribution around the head and consequently the precision of the source localization is significantly affected by several parameters. One of these is the configuration of the surface at which the magnetic field distribution is measured. Another is the component of the magnetic field vector which is recorded. Up to now the commonly used measurement procedure has been to fix the pick-up coil of the gradiometer normal to the scalp at positions as near to the head as possible. Williamson et al. (1984) used a spherical recording surface. The points in favour of this procedure are 3-fold. The first is that a spherical recording surface is consistent with present models of the head which are also spherical. The second in favour is that a spherical surface is convenient because only two angular variables have to be controlled. The third point is that positioning of the gradiometer can be carried out with a precision better than 0.5°. The first point mentioned is, of course, only valid when the head is modelled as a set of concentric spheres. When the electrical conductivities in several of the spherical compartments are different but homogeneous and isotropic within each compartment (i.e., have the same value in all directions), the radial (normal) component of the magnetic field does not reflect the influence of the volume conductor. A radially oriented dipole in such a volume conductor does not contribute to the magnetic field. However, the shape of a human head is not spherical. Because of this latter fact, the normal component of the magnetic field may be influenced by the shape of the volume conductor. Current dipoles which, in a first-order approximation, can be considered to be radial may also contribute to the magnetic field outside the head. Since the order of magnitude of these contributions to the total magnetic field is not quantitatively evaluated, it cannot be said in advance whether the spherical recording surface is the best choice.

In this study the influence of the actual anatomical shape of the volume conductor on the magnetic field distribution around the head is investigated. Therefore, a realistically shaped multi-compartment model of the head was constructed from magnetic resonance (MR) images.

Method

The model of the head consists of 3 homogeneous isotropic compartments representing the brain, the skull and the scalp. The model of the source used is a current dipole, which is located in that part of the brain which corresponds to the visual cortex, since visual evoked magnetic fields were a subject of earlier study (Kouijzer et al. 1985).

The purpose of this study was to answer the following questions with the help of simulations, using the above-mentioned model.

Which recording surface must be chosen in order to obtain a minimum contribution of the volume currents? As options we considered a plane, a section of a sphere (i.e., a sphere concentric with the sphere which is the best possible fit for the head) and a surface equidistant from the actual scalp, which means that this surface follows the contours of the head.

Which component of the magnetic field vector is least affected by the volume currents?

What influence on the MEG maps can be expected as a result of an inaccuracy in the orientation of the magnetic field detector?

The numerical calculations were based on the integral equations derived respectively by Barnard et al. (1967) and Geselowitz (1970). These equations show that the contribution of the volume currents in a piecewise homogeneous, isotropic volume conductor can be considered equivalent to the influence of secondary sources which lie at the interface between regions of different conductivities. The orientation of these secondary sources is normal to the interfaces and the value of the secondary sources is linearly proportional to the electrical potential at that location. The magnetic fields due to these secondary sources are added to the magnetic field due to the primary source (i.e., the single current dipole) to set up the observed magnetic field distribution.

To compute the magnetic field distribution and

the electrical potential distribution numerically, the integral equations mentioned above must be approximated by summations. The usual approach to this problem is to represent the surfaces involved by many small triangles and to assume that the potential is constant over each triangle. The more triangles that are taken the better the approximation of the integral equation will be.

Model

The source is modelled by a single-current dipole. In order to construct the model of the head, data of 22 cross-sectional MR images of a human head were recorded, ranging from the top of the head to 10 mm below the mandible. On the contours of each cross-section a discrete number of points were chosen, being the vertices of the triangles describing the boundaries of the compartments. The potential distribution on an interface near the current dipole varies more than on a more remote interface. However, in the discrete computations the potential on each triangle was assumed to be constant. In order to increase the accuracy, the points were arranged in such a way that the area of any triangle was small in the section of the head near the source location (i.e., the visual cortex) and larger at greater distances. The triangulated model is shown in Fig. 1a, 1b and 1c, representing the boundaries of, respectively, the scalp, skull and brain tissues. The number of vertex points on each interface was 288. The conductivities of the compartments which represented the brain and the scalp were 0.33 siemens/m (Sm^{-1}); these values correspond with those reported elsewhere (Geddes and Baker 1967). For the skull a conductivity of 0.033 Sm^{-1} was chosen although in the literature the conductivity for bone varies between 0.0042 Sm^{-1} and 0.0063 Sm^{-1}. These data indicate that in this study the value of the conductivity of the skull was too high by a factor of 10. This high conductivity value was chosen because the numerical procedure used was found to magnify errors due to the discrete computations when the ratio of the conductivities in the successive compartments was large. Of course, these computational errors can always be diminished by augmenting the number of triangles. However, this procedure leads to a practical problem since the number of discrete points needed to obtain an accuracy of 5% in the final field distribution would result in a CPU time in the order of 200 h for the DEC-20 computer used for the computations. The amount of computational work can be substantially decreased by making use of

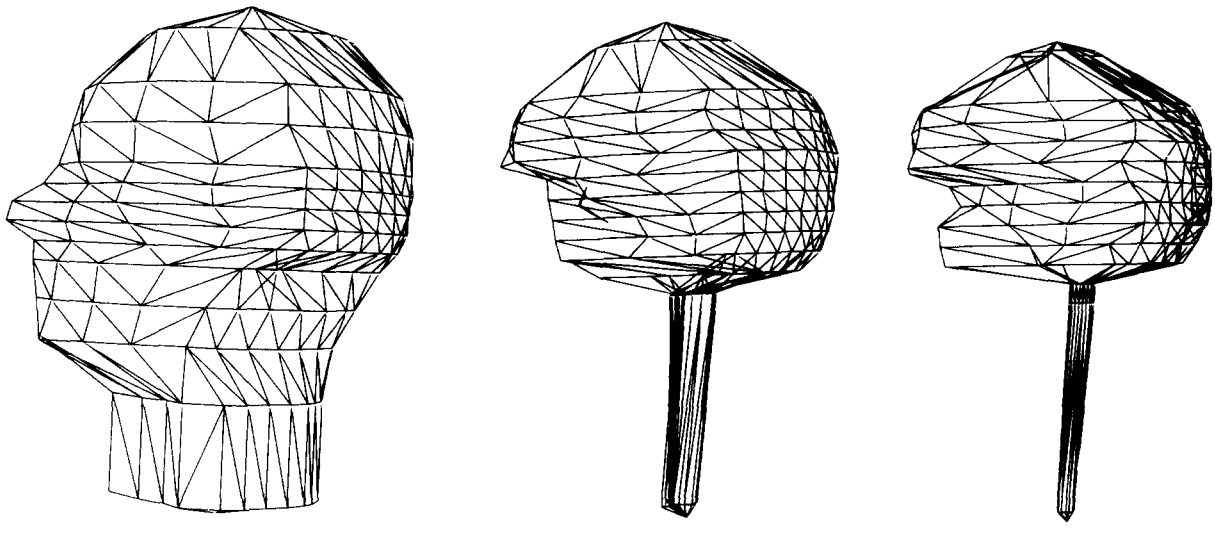

Fig. 1. The triangulated model of the head: scalp (a), skull (b) and brain (c), used to simulate the influence of the volume conductor on the magnetic field distribution outside the head.

the Richardson extrapolation technique, as described elsewhere (Meijs et al. 1987). Nevertheless, the present study demonstrates the usefulness of the new model of the volume conductor. If a more realistic value of the conductivity of the skull is taken, the secondary sources at the brain/skull interface will have higher values. The secondary sources at the skull/scalp interface, having an opposite sign, will have higher values as well. It is very difficult to predict the resulting magnetic field distribution quantitatively.

We are mainly interested to know in which recording surface the contribution of the secondary sources to the magnetic field, relative to the contribution of the primary sources, is minimal. It is not to be expected that the answer to this qualitative question depends on the fact that a higher value for bone tissue is taken. The results obtained will only be more or less pronounced.

The recording surface

When carrying out biomagnetic measurements a matrix of grid points is necessary in which the magnetic field is measured. The geometrical surface on which all grid points are situated is called the recording surface.

In order to investigate which recording surface offers the best choice for measuring the magnetic field, the latter was calculated on various surfaces, viz., a plane, a sphere and a surface which followed the contours of the head. The coordinate system used is depicted in Fig. 2.

The plane chosen was y = constant at a distance of 18 mm to the nearest point on the scalp. In practice this distance was determined by the distance between the bottom of the cryostat and the pick-up coil of the gradiometer.

The chosen sphere segment was concentric with a sphere which was the best possible fit for the head and especially for the section at the back of the scalp. This fitting was carried out by means of a least squares fitting procedure (Numerical Algorithms Group Library, NAGLIB: routine E04FCF); the resultant sphere is represented in Fig. 2. The recording sphere was tangent to the plane mentioned above.

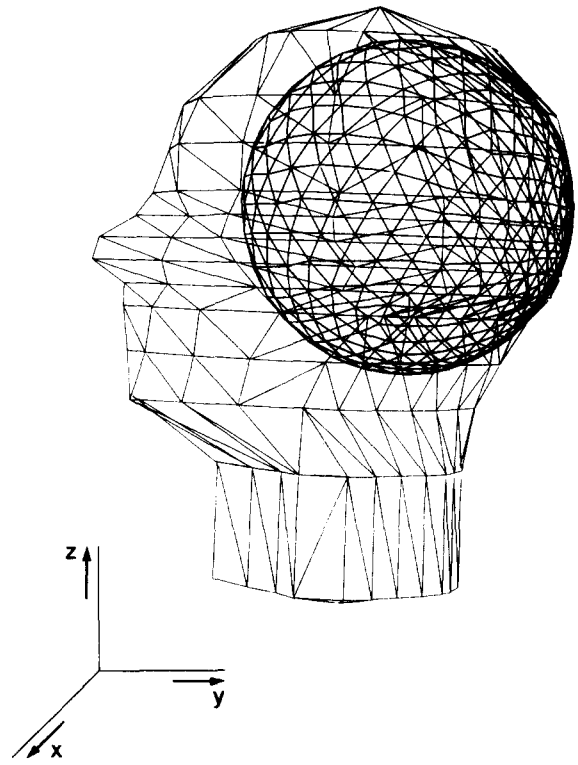

Fig. 2. The coordinate system used with respect to the triangulated model of the head. In this model the sphere is shown which is the best possible fit for the head, especially for the section near the visual cortex.

The recording surface which followed the contours of the head was constructed from the triangulated model of the outer surface of the scalp. At each vertex on this surface a normal vector was constructed corresponding to the average of the normal vectors of all adjacent triangles. The grid points in the 'head-following' recording surface were obtained by taking points at a distance of 18 mm from the vertices along these normal vectors.

The components of the magnetic field studied here were adapted to the recording surface used. When the normal unit vector in each point on the surface chosen is called $\vec{n}$ then the other unit vectors are defined by $\vec{t}_2 = \vec{e}_z \times \vec{n}$ and $\vec{t}_1 = \vec{t}_2 \times \vec{n}$, where $\vec{e}_z$ is the unit vector in the z direction. This means that $(\vec{n}, \vec{t}_1, \vec{t}_2)$ is a local cartesian coordinate system (see Fig. 3). The components of the magnetic field studied were respectively in the $\vec{n}$, $\vec{t}_1$ and $\vec{t}_2$ directions.

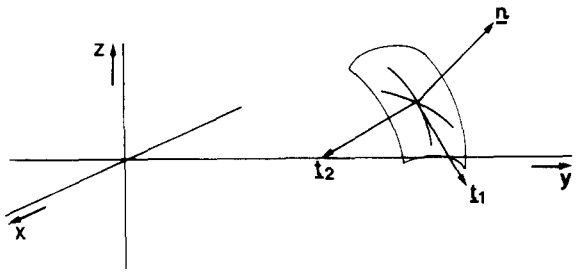

Fig. 3. The local cartesian coordinate system. The components of the magnetic field studied are respectively in the $\vec{n}$, $\vec{t}_1$ and $\vec{t}_2$ directions.

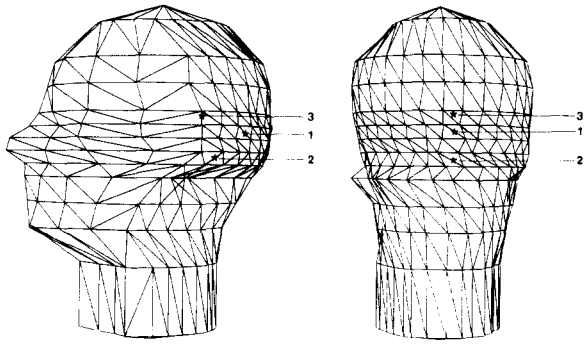

Fig. 4. The magnetic field distribution around the head is simulated taking the current dipole in 3 distinct locations. These are indicated by asterisks. The orientation of the dipole is taken respectively in the x, y, or z direction as depicted in Fig. 2. a: side view. b: rear view.

Results

The single current dipole which acts as the primary source was placed at 3 distinct locations in that section of the brain which reflects the visual area of the cortex. The source locations were so chosen that from a mathematical point of view different sites were chosen. These source locations could provide an insight into the location dependency of the dipole on the generated magnetic field pattern. The dipole locations are depicted in Fig. 4. The orientation of the dipole was taken in the x, the y and the z directions. The strength of the current dipole was 5×10^{-6} A. All 3 components of the magnetic field were calculated on all 3 recording surfaces for all 3 locations and all 3 orientations of the dipole. Thus a total of 81 simulations were carried out. The resulting field patterns are presented by means of isofield-component lines in a plane. The projection in the case of both the sphere and the 'head-following' surface is such that the distances in both the $\vec{t}_1$ and $\vec{t}_2$ directions remain the same. The projected representations of the grid points on the various recording surfaces are given in Fig. 5.

The resulting magnetic field patterns are given in a series of 3 maps, see Fig. 6, in order to

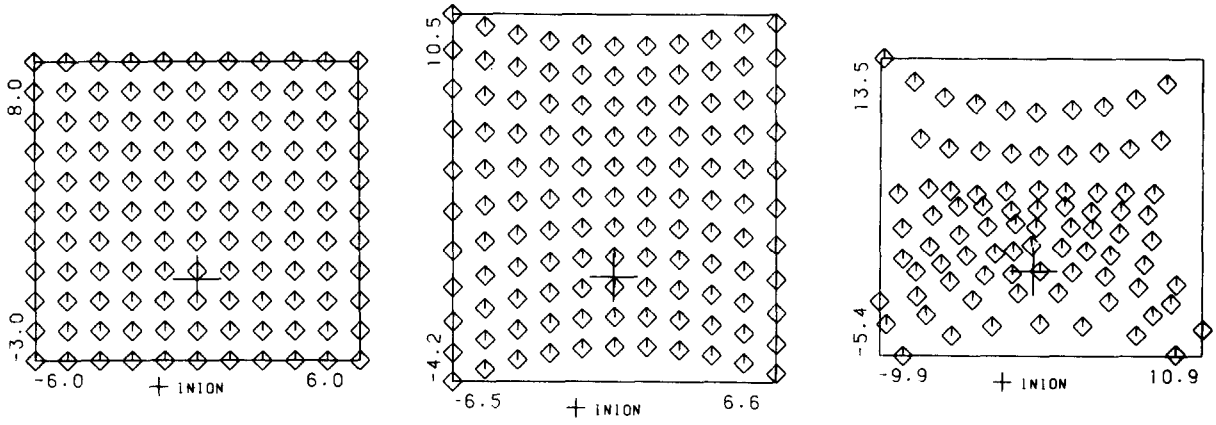

Fig. 5. The projection of the grid points in which the magnetic field is calculated (dimensions are presented in cm). a: the grid points are situated on a plane. b: the grid points are situated on a sphere. c: the grid points are on a surface which follows the contours of the head.

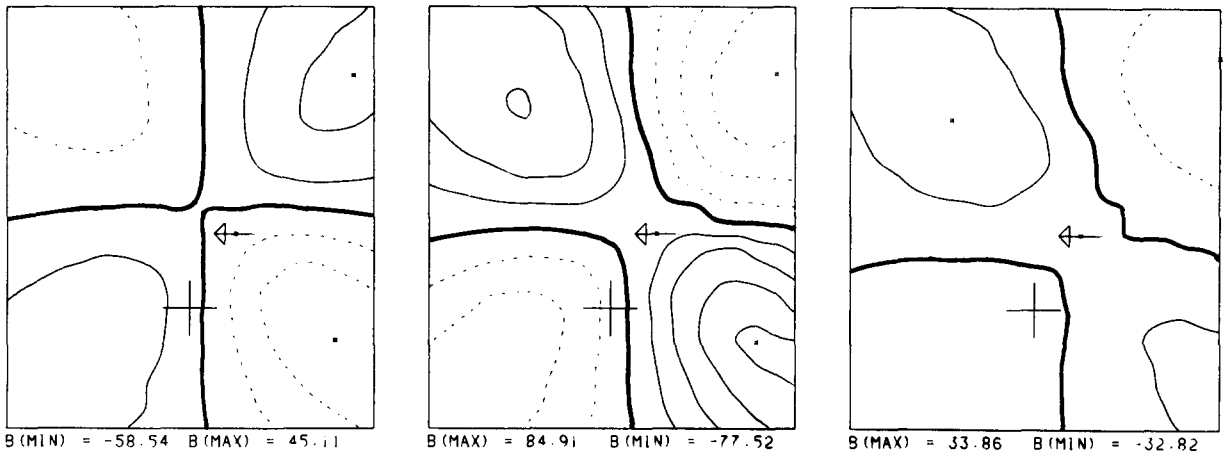

Fig. 6. Simulated isocontour maps of the magnetic field component in the $\vec{t}_1$ direction. The recording surface is a sphere. The current dipole is source number 1, as indicated in Fig. 4. This dipole points in the x direction. The arrow indicates the projected direction and position of the dipole; the distance beneath the surface of the recording sphere is 3.8 cm. The cross indicates the inion. The dimensions of the map are 12.5 cm × 15 cm. The separation between successive contours is 20 pT. Solid lines indicate that the field is leaving the head, dotted lines indicate that the field is entering the head. The line interconnecting the points where the magnetic field component is zero is given by a thick line. The first map of the series represents the contribution of the primary source only, the second one the exclusive contribution of the secondary sources and the third the superposition of the first two (i.e., the distribution of the total magnetic field component in the $\vec{t}_1$ direction). Note that the contribution of the secondary sources is even larger than that of the primary source.

separate the contribution of the primary source from that of the sencondary sources. The third map of each series is a simulation of the map which can be obtained from experimental measurements. In order to be able to compare the fields generated by the primary and secondary sources the ratio of the difference between the extremes found in the map generated by the current dipole only and the extremes in the map generated exclusively by the secondary sources will be expressed in percentages.

(1) Investigation of the maps of the tangential components of the magnetic field on all surfaces mentioned

The contribution of the primary source to the various tangential components of the field showed diverse patterns. Depending on the orientation of the dipole we obtained dipolar, quadrupolar and circular patterns. In all cases we found that the contribution of the secondary sources to the tangential components strongly counteracted the contribution of the primary source. Therefore the resulting total tangential field components were strongly influenced by the secondary sources. This typical behaviour is demonstrated in Figs. 6 and 7.

(2) Study of the behaviour of the normal component of the magnetic field (B_n) for all 3 types of recording surface

(2.1) The recording surface is a plane. When the dipole is pointing in the x or z direction (i.e., tangential to the recording plane), the primary source generates a dipole pattern (i.e., two extremes and the line indicating zero value between these extremes). In these cases the contribution of the volume currents is substantial and counteracts the contribution of the source. A demonstration of this behaviour is given in Fig. 8. If the dipole is pointing in the y direction the maps generated by the primary source is blank and the pattern of the maps generated by the volume currents is not recognizable.

(2.2) The recording surface is a sphere. When the dipole is pointing in the x or z direction the distribution of B_n on the spherical recording surface always shows a dipolar pattern, as shown in Fig. 9a. The contribution of the secondary

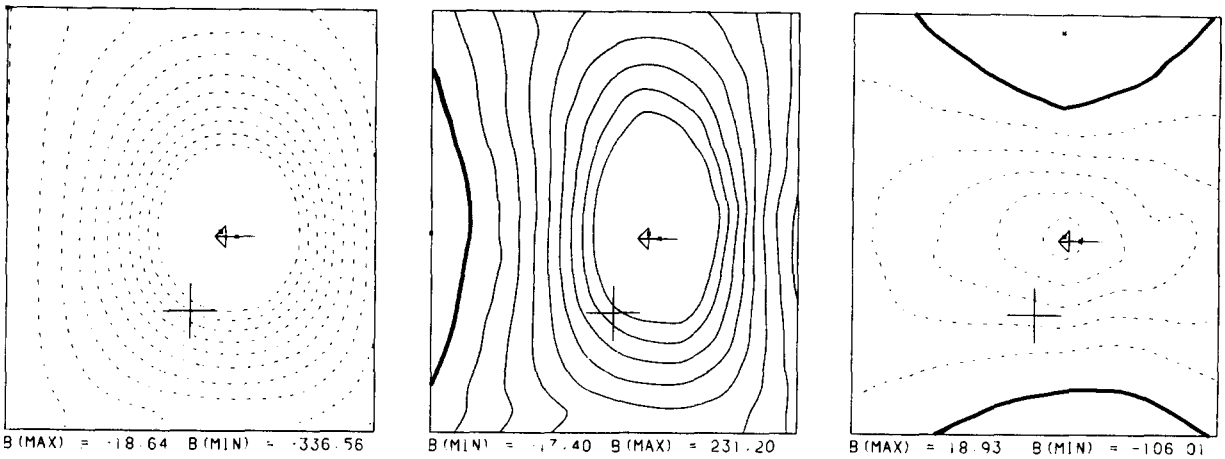

Fig. 7. As Fig. 6, but the field component chosen is in the t_2 direction. The recording surface is a plane. The dipole (number 1) is located 4.0 cm beneath the plane. The dimensions of the map are 12 cm × 12 cm.

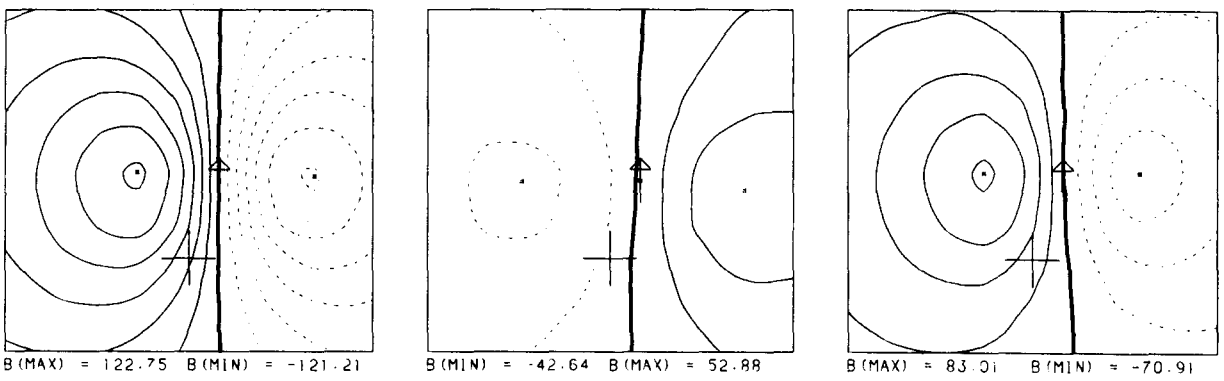

Fig. 8. As Fig. 6, but the field component is normal to the recording surface, which is a plane. The dipole is again dipole number 1. The dimensions of the map are 12 cm × 12 cm. Note that the secondary sources counteract the field generated by the primary source.

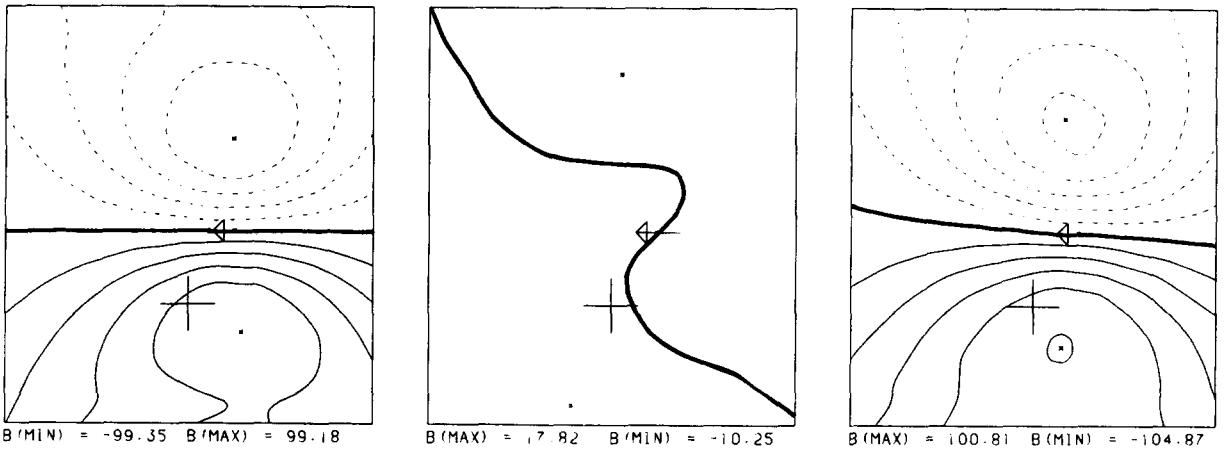

Fig. 9. As Fig. 6. The field component is normal to the recording surface, which is a sphere. The dipole is dipole number 1, pointing in the z direction. Note that the contribution of the volume currents is small.

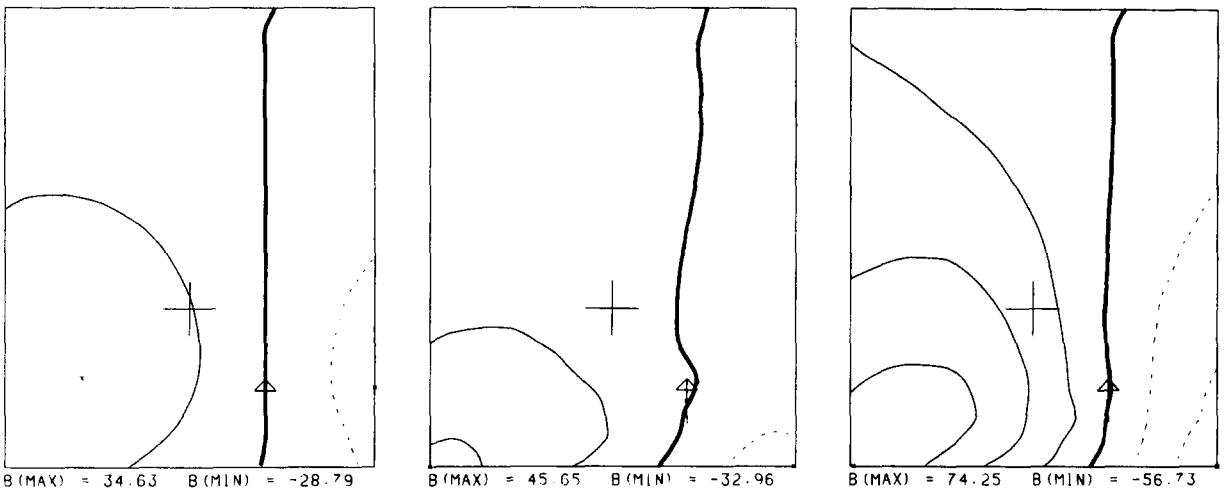

Fig. 10. As Fig. 9, but the dipole is dipole number 2, pointing in the z direction. The source depth is 4.9 cm. Note that the contribution of the volume currents relative to those of the primary source is large. The contribution of the volume currents increases with source depth.

sources is very small (less than 10%) for source number 1 (Fig. 9). For sources numbered 2 and 3, which are located deeper within the brain, this influence is larger. For example, the ratio between the contributions of the primary and secondary sources for dipole number 2, orientated in the z direction is 100%. The contribution of the secondary sources reinforces that of the primary source (Fig. 10).

A dipole pointing in the y direction has in first order approximation surface for the chosen source locations. The amplitudes of B_n generated by the primary source are small (Fig. 11). However, the values of the final B_n may have the same order of magnitude, as is the case when the dipole is in the x or z direction. For example, if one looks at dipole number 2 pointing in the y direction it can be seen that the difference between the two extremes equals 70 picotesla (pT) while if the same dipole is pointing in the x or z direction this value is 131 pT.

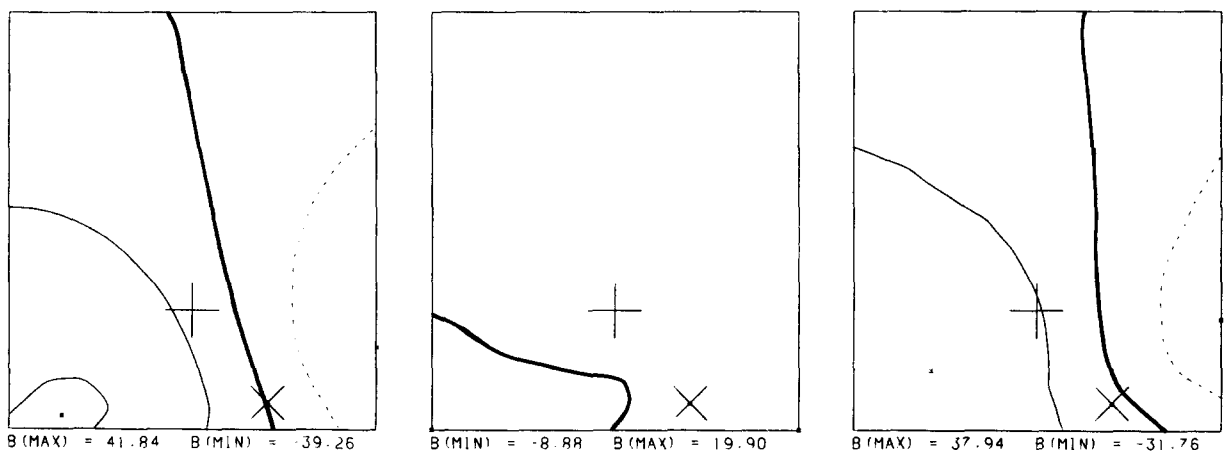

Fig. 11. As Fig. 9, but the dipole is dipole number 2, pointing in the y direction (approximately radial in the sphere which acts as recording surface).

(2.3) The recording surface follows the contours of the head. If the dipole is pointing in the x direction the distortion of the dipolar pattern of B_n, generated by the primary source, becomes apparent. The secondary sources counteract the contribution of the primary source (Fig. 12). Their influence increases with source depth, and the ratio of the contribution of the primary and secondary sources is, for example, for source number 3, 50%. If the dipole is pointing in the z direction the same conclusions as in the case of the dipole in the x direction can be made. The only difference is that the secondary sources reinforce the contribution of the primary source.

If the dipole is pointing in the y direction, the primary source does not give a recognizable pattern, neither do the secondary sources. However, the values of the extremes of the final distribu-

TABLE I

Listed in Table I: (1) The direction of the magnetic field component recorded (see Fig. 3). (2) The recording surface, used in the simulation. (3) The direction of the dipole (see Fig. 3). (4) The dipole location, where the dipole numbers correspond with those used in Fig. 5. (5) The magnetic field due to the primary source: B_∞. Listed is the difference between the maximum and minimum of B_∞ mapped. (6) The resulting total magnetic field B_n. Listed is the difference between the maximum and minimum of B_n mapped.

Component magnetic field (1)	Recording surface (2)	Dipole direction (3)	Dipole number (4)	Primary field B_∞ (5) (in pT)	Total magnetic field (6) (in pT)
$\vec{t}_1, \vec{t}_2$	all	all	all	*	*
$\vec{n}$**	plane	x	1	242	163
			2	90	60
			3	67	22
		y	1	0	30
			2	0	31
			3	0	7
		z	1	244	153
			2	91	51
			3	68	20
	sphere	x	1	198	206
			2	66	112
			3	22	40
		y	1	55	42
			2	81	70
			3	9	19
		z	1	195	192
			2	63	131
			3	20	24
	'head-following'	x	1	240	212
			2	143	130
			3	53	36
		y	1	89	46
			2	110	83
			3	44	20
		z	1	214	206
			2	85	114
			3	30	34

* Because the tangential component of B_∞ showed various isomagnetic field patterns, no meaningful number can be given; the total magnetic field is always a small fraction of B_∞.

** Using a dipole in the x or z direction all field distributions show dipolar patterns. For the 'head-following' surface this dipolar pattern is distorted (Fig. 12), which has to be expected since both the shape and the normal direction on this surface depend on the actual shape of the head.

Fig. 12. As Fig. 6, but the field component is normal to the surface which follows the contours of the head. The dipole is dipole number 1, pointing in the x direction.

tions of B_n are not negligible. For example when dipole number 3 is considered, investigation of the differences between the extremes shows that this value equals 20 pT if the dipole is pointing in the y direction, being approximately radial. The difference between the extremes is 35 pT if the dipole is pointing in the x or z direction, which is approximately tangential.

In Table I we have listed a schematic summary of the results discussed in this section.

Conclusions

Five main points can be made as will be discussed in the next section:

(i) It is not recommended to measure the tangential components of the magnetic field, since the contribution of the primary source may show intricate types of pattern and the total magnetic field is strongly influenced by the contribution of the secondary sources.

(ii) The use of a plane as a recording surface is a poor choice, as can be seen by noting the contribution of the secondary sources to the normal components of the total magnetic field.

(iii) The best choice is to measure the distribution of the magnetic field component perpendicular to the sphere which is the best fitted for the local curvature of the head.

(iv) For eccentrically located primary sources small changes in the radius of the sphere mentioned in (iii) do not change the magnetic field distribution noticeably. This means that for superficial sources the recording surface of a multi-array SQUID magnetometer can be constructed on the spheric concave bottom of a cryostat.

(v) Forward calculations show that the magnetic field distribution resulting from a primary source located deep within the brain based on a spherical model of the head does not coincide with that based on the more realistically shaped model of the head.

Discussion

The contribution of the secondary sources to the distribution of the normal component of the magnetic field in a plane is relatively large (up to 80%), counteracting the contribution of the primary sources. Thus we must discuss the remaining possibilities: the normal component on the 'head-following' surface and the normal component on the sphere.

For the head-following surface the contribution of the primary source to B_n is slightly larger than for the sphere. This can be expected because this surface is as near to the source as possible. On the other hand, on the spherical surface the contribution of the secondary sources is smaller.

An important argument in favour of a particular choice of a recording surface is dictated by the degree of accuracy which can be accomplished in practice when measuring in a particular direction at a point on that surface. Displacements in the

orientation of the pick-up coil of the gradiometer with respect to the normal on the head give rise to a contribution of the tangential component to the field measured. It is impossible to measure exactly the normal component on the head. Inspecting the results presented in this study one can see that the tangential component of the magnetic field on the head-following surface is of the same order of magnitude as the normal component of this field. This means that a displacement of 10° in the orientation of the pick-up coil could give a tangential component having a value in the order of 20% of that of the normal component. Because the sensitivity of the magnetic field measurement to the detector orientation turns out to be so large, a measuring method which is shown to be inaccurate in the sensor orientation has to be avoided.

In the case where the recording surface is a sphere the sensitivity to the detector orientation is, for the same reasons as mentioned above, as large as in the case of the head-following surface. However, it is possible to measure the normal direction on a sphere with a high degree of accuracy. By means of the least squares fitting procedure the recording sphere can be computed for each individual subject (Romani and Leoni 1984). In order to estimate the sensitivity of the magnetic field distribution to the sphere obtained with this sphere-fitting procedure, the centre of the sphere was moved 1 cm in the positive z direction and some of the simulations were repeated. The ratio between the contribution of the secondary and primary sources is merely enhanced by a factor in the order of 5% if the eccentrically located dipole was taken (dipole number 1).

As a result of all the arguments mentioned above the spherical recording surface is recommended. The normal component of the magnetic field should be recorded on this surface. In the case of an eccentric dipole this means that the radially oriented dipole gives no substantial contribution to the field and the secondary sources give no substantial contribution to the normal component of the field. However, for sources located more deeply within the brain (sources numbered 2 and 3) the influence of the volume currents on the normal component of the magnetic field is apparent, as is the contribution to B_n due to a radially oriented dipole.

It can be deduced from the latter that a volume conductor model consisting of spheres, which are concentric with the best local fitting sphere in the head, is not an adequate model for sources located more deeply within the brain. This follows directly from the fact that the secondary sources play an important role in the component of the magnetic field normal to the concentric spheres instead of providing a zero contribution. However, if the dipole is chosen eccentrically (dipole number 1) the use of the multi-sphere model mentioned above does not lead to large discrepancies (Meijs et al. 1985), but if the sources are located deeper within the brain, it does. This is in accordance with the experiments of Barth et al. (1986), who implanted a dipolar current source in a human cranium filled with a conductive salt jelly. The source was positioned at the right anterior temporal region. The measured MEG maps showed a dipolar configuration but the shape and relative amplitude of the extrema differed from those of the sphere. The degree of the distortion of the magnetic field pattern also increased with source depth.

The present study has an important practical application, since it provides a guideline on how to arrange the pick-up coils in a multi-sensor magnetometer. In such a device the bottom of the cryostat on which the gradiometers are positioned should have a spherical concavity. The radius of this concavity is such that it encloses everybody's head at all locations although its radius will not be adjustable for a particular head. The spherical arrangement of the pick-up coils within such a cryostat is merely an approximation of the locally best fitting spherical recording surface. Therefore it was necessary to estimate the influence of the radius of the recording sphere on the magnetic field pattern B_n. In order to do so the radius of the recording sphere was enhanced by 1 cm, the distance from the head was kept at 18 mm. In the case of the eccentric dipole the ratio of the contribution between the primary and secondary sources was not noticeably changed. This means that at least for a superficial source a cryostat having a bottom with a spherical concavity with a fixed radius will provide a measuring grid which is appropriate for localizing the source in a variety of human heads.

A realistically shaped model of the head is complicated. The present data demonstrate that the magnetic field distribution differs from that based on a concentric spheres model. The deviation increases with source depth. In the near future investigations will be done to determine whether a simplification of the realistically shaped multi-compartment model of the head described here can act also as an adequate model.

Many of the outstanding questions relating to source localization involve sources which are deep within the brain. In a model consisting of concentric spheres current dipoles in the midpoint of the volume conductor do not contribute to the magnetic field at all. This means that if the spherical model turned out to be an adequate model to describe sources deep within the brain, the magnetic field could not be used to localize, or even measure, these deeply located sources. Thus the fact that a spherical model is an adequate model for superficial dipoles (providing a simple localization method) combined with the fact that this spherical model is not an adequate model when the dipole is situated deep within the brain may be an advantage with respect to localization possibilities by means of magnetic measurements.

Résumé

Distribution du champ magnétique généré par une source de courant dipôlaire située dans un modèle compartimenté de la tête proche de la forme réelle

On a simulé la distribution du champ magnétique autour de la tête en utilisant un modèle compartimenté de tête proche de la forme réelle. Ce modèle est basé sur des images de résonance magnétique. Les trois compartiments correspondent au cerveau, au crâne et au scalp. La source est représentée par un dipôle de courant situé dans le cortex visuel. La distribution du champ magnétique due à cette source et celle due aux courants en volume sont calculées séparément. Ces simulations ont été faites afin de déterminer quelle matrice de points de la grilles sont valables comme grille de mesure. On a examiné comme possibilités des points de grille situés soit dans un plan, soit selon une surface épousant les contours de la tête, soit selon une sphère. Cette sphère était concentrique celle qui correspondait le mieux à la forme de la tête. Si l'on prend en compte la contribution relative des courants en volume et l'exactitude que l'on peut attendre pour la position du détecteur de champ magnétique, on peut conclure que le meilleur choix est de mesurer la composante normale du champ magnétique en des points de la surface sphérique. Les résultats de cette étude montrent aussi que la distribution du champ magnétique fondées sur un modèle compartimenté proche de la réalité diffère de celles basées sur un modèle fait de sphères concentriques. Dans le modèle sphérique de la tête, on ne peut attendre de contribution des courants de volume à la composante du champ normal de la sphère. La différence entre les résultats obtenus et avec l'un et l'autre modèle à deux volumes conducteurs augmente avec la profondeur de la source.

References

Barnard, A.C.L., Duck, J.M., Lynn, M.S. and Timlake, W.P. The application of electromagnetic theory to electrocardiology, II. Biophys. J., 1967, 7: 463–491.

Barth, D.S., Sutherling, W., Engel, Jr., J. and Beatty, J. Neuromagnetic evidence of spatially distributed sources underlying epileptiform spikes in the human brain. Science, 1984, 223: 293–296.

Barth, D.S., Sutherling, W., Broffman, J. and Jackson, B. Magnetic localization of a dipolar current source implanted in a sphere and a human cranium. Electroenceph. clin. Neurophysiol., 1986, 63: 260–273.

Cohen, D. and Cuffin, B.N. Demonstration of useful differences between magnetoencephalogram and electroencephalogram. Electroenceph. clin. Neurophysiol., 1983, 56: 36–51.

Geddes, L.A. and Baker, L.E. The specific resistance of biological material, a compendium of data for the biomedical engineer and physiologist. Med. biol. Engng, 1967, 5: 271–293.

Geselowitz, D.B. On the magnetic field generated outside an inhomogeneous volume conductor by internal sources. IEEE Trans. Magn., 1970, Mag-6: 346–347.

Kouijzer, W.J.J., Stok, C.J., Reits, D., Peters, M.J., Dunajski, Z. and Lopes da Silva, F.H. Neuromagnetic fields evoked by a patterned on-offset stimulus. IEEE Trans. biomed. Engng, 1985, BME-32: 455–458.

Meijs, J.W.H., Peters, M.J. and Oosterom, A. van. Computation of MEGs and EEGs using a realistically shaped multicompartment model of the head. Med. biol. Engng Comput., 1985, 23 (Suppl. Part 1): 36–37.

Meijs, J.W.H., Peters, M.J., Oosterom, A. van and Boom, H.B.K. The application of the Richardson extrapolation in simulation studies of EEGs. Med. biol. Engng Comput., 1987, in press.

Romani, G.L. and Leoni, R. Localization of cerebral sources by neuromagnetic measurements. In: H. Weinberg, G. Stroink and T. Katila (Eds.), Biomagnetism: Applications and Theory. Pergamon Press, Vancouver, 1984: 205–220.

Stok, C.J., Kouijzer, W.J.J. and Peters, M.J. Source localization based on EEGs and MEGs. In: H. Weinberg, G. Stroink and T. Katila (Eds.), Biomagnetism: Applications and Theory. Pergamon Press, Vancouver, 1984: 283–288.

Weinberg, H., Brickett, P., Coolsma, F. and Baff, M. Topography of simulated MEG and EEG generated by multiple intracranial dipoles. In: H. Weinberg, G. Stroink and T. Katila (Eds.), Biomagnetism: Applications and Theory. Pergamon Press, Vancouver, 1984: 273–277.

Williamson, S.J., Pellizone, M., Okada, Y., Kaufman, L., Crum, D.B. and Marsden, J.R. Magnetoencephalography with an array of SQUID sensors. In: H. Collan, P. Berglund and M. Krusius (Eds.), Proc. 10th Int. Cryogenic Engineering Conference, Helsinki. Butterworth, London, 1984: 339–348.